PROCEEDINGS OF THE ROYAL SOCIETY A

Proc. R. Soc. A (2005) **461**, 2071–2098
doi:10.1098/rspa.2005.1507
Published online 6 June 2005

The optical singularities of bianisotropic crystals

By M. V. Berry

H. H. Wills Physics Laboratory, Tyndall Avenue, Bristol BS8 1TL, UK

The electric and magnetic polarization states for plane waves in arbitrary linear crystals, in which each of $\boldsymbol{D}$ and $\boldsymbol{B}$ is coupled to both of $\boldsymbol{E}$ and $\boldsymbol{H}$, can be characterized by their typical singularities in direction space: degeneracies, where two refractive index eigenvalues coincide; C_{e} and C_{m} points, where the electric or magnetic field is circularly polarized; and L_{e} and L_{m} lines, where either field is linearly polarized. The well-known 4×4 matrix formalism, expressed in terms of the stereographic projection of directions, enables extensive numerical and visual exploration of the singularities in the general case (which involves 65 crystal parameters), incorporating bianisotropy, natural and Faraday optical activity, and absorption, as well as special cases where one or more effect is absent. For crystals whose anisotropy is weak but which are otherwise general, an unusual perturbation theory leads to a powerful 2×2 formalism capturing all the essential singularity phenomena, including the principal feature of the general case, namely the separation between the electric and magnetic singularities.

Keywords: degeneracies; polarization; electromagnetism

1. Introduction

Bianisotropic crystals are the most general linear local electromagnetic materials (Kong 1975), in which each of the field vectors $\boldsymbol{E}$ and $\boldsymbol{H}$ is coupled tensorially to both of the associated vectors $\boldsymbol{D}$ and $\boldsymbol{B}$. Such materials have been the subject of considerable recent interest; one reason is that they can be created as metamaterials: composites of more conventional materials in which $\boldsymbol{E}$ is coupled to $\boldsymbol{D}$ alone and $\boldsymbol{H}$ is coupled to $\boldsymbol{B}$ alone (Weiglhofer & Lakhtakia 2003).

General bianisotropic coupling incorporates many different polarization phenomena, including genuine electric-magnetic cross-coupling effects, conventional electric and magnetic biaxial anisotropy, Faraday effects, and natural optical activity, as well as the absorptive counterparts of all these if there is dissipation in the material. Thus, bianisotropy implies a many-dimensional crystal space (described by 65 real parameters, as we will see in §2). Without a common framework to describe the polarization states, navigation in this 'crystal space' is difficult. It is my purpose here to provide such a framework for plane waves, by focusing on the singularities in the patterns of electric and magnetic polarizations as functions of the wavevector direction $\boldsymbol{s}$ (a unit vector), for each

Received 25 January 2005
Accepted 25 April 2005

type of material. The singularities to be considered are generic: those that occur typically, that is stably under variations of the constitutive parameters characterizing the crystal.

As the fundamental fields we choose $\boldsymbol{D}$ and $\boldsymbol{B}$, rather than $\boldsymbol{E}$ and $\boldsymbol{H}$ or $\boldsymbol{E}$ and $\boldsymbol{B}$, because $\boldsymbol{D}$ and $\boldsymbol{B}$ are always transverse to the wave direction $\boldsymbol{s}$, so, as is well known (Kong 1974), the 6×6 matrix formalism can be reduced to 4×4 (§3). $\boldsymbol{D}$ and $\boldsymbol{B}$ can be represented by a single four-component vector, but we choose to consider the singularities of $\boldsymbol{D}$ and $\boldsymbol{B}$ separately. This neglect of the Lorentz symmetry, in which a change of inertial reference frame would mix the components of $\boldsymbol{D}$ and $\boldsymbol{B}$, is appropriate because we are considering monochromatic plane waves in a uniform medium, providing a natural rest frame, so relativity is irrelevant (although we note the interesting fact that motion can induce bianisotropy and even a negative refractive index; see Mackay & Lakhtakia 2004).

An approach to crystal optics based on singularities was recently initiated and explored in detail for the case of purely electrical anisotropy (Berry & Dennis 2003). There are three types of singularity in the (always-transverse) vector $\boldsymbol{D}(\boldsymbol{s})$: degeneracies, that is directions (points in $\boldsymbol{s}$ space) in which the two (generally complex) refractive indices coincide; C points in $\boldsymbol{s}$ space, where either of the two states is purely circularly polarized; and L lines in $\boldsymbol{s}$ space, where either polarization is purely linear. The degeneracies are branch points for absorbing crystals, and conical points for transparent non-chiral crystals. In the absence of chirality, the C points and the degeneracies coincide.

In the bianisotropic case, the same singularities occur, but with two main complicating factors. First, the singularities of the electric and magnetic fields (§4) are in general different, so both must be considered. Second, with the transverse fields $\boldsymbol{D}$ and $\boldsymbol{B}$ the formalism involves 4×4 matrices rather than 2×2 matrices.

The singularity structures for different crystals will be illustrated by numerical calculations based on a sufficiently general representative crystal space in which the various effects are described by six parameters and displayed visually using a common set of pictorial conventions (§5).

Several special cases are considered in §6. The most important is transparent crystals (§6*a*); neglect of absorption means that the relevant matrices are Hermitian, with dramatic effects on the singularity structure. Another special case is that of Lorentz reciprocity (Kong 1975; Krowne 1984): an even spectrum (§6*b*), in which the (possibly complex) refractive indices are invariant under the antipodal transformation $\boldsymbol{s}\rightarrow-\boldsymbol{s}$; this occurs, for example, when the crystal is optically inactive. Finally, there is the special case of doubly anisotropic crystals (§6*c*), in which $\boldsymbol{D}$ is anisotropically coupled to $\boldsymbol{E}$, and $\boldsymbol{B}$ is anisotropically coupled to $\boldsymbol{H}$, but there is no cross-coupling; this introduces the simplification that the 4×4 matrices can be reduced exactly to 2×2 ones. In the special case of non-chiral double anisotropy, the degeneracies are slightly separated from the C points, even though the governing matrices are complex symmetric—behaviour contrasting with the purely electric chiral situation, in which the two singularities always coincide (Berry & Dennis 2003).

A major simplification, which I hope will have applications beyond the present study of singularities, occurs when all anisotropies, including bianisotropic

cross-couplings, are weak (§7). Then the general 4×4 matrix formalism can be reduced to one involving 2×2 matrices and the vector $\boldsymbol{D}$ alone. This version of perturbation theory turns out to be surprisingly powerful even for crystals that are not very weak. The reduction to 2×2 matrices is an enormous simplification, enabling analytical description of the singularities, in particular, the central feature that bianisotropy brings, namely the separation of the electric and magnetic singularities (§8).

As in our earlier work on purely electric anisotropy (Berry & Dennis 2003), the term 'crystal' will here refer to any material that is uniform of the scale of the wavelength, and so includes liquid crystals, plastics such as overhead-projector transparency foil (Berry *et al.* 1999; Berry & Dennis 2004), glass, microscopic composites, magnetized plasmas, etc.

2. Constitutive relations

For the plane wave we will be considering, travelling in a direction described by the unit wavevector $\boldsymbol{s}$, the physical electromagnetic fields can be written

$$\boldsymbol{D}_{\mathrm{phys}}(\boldsymbol{r},t)=\mathrm{Re}[\boldsymbol{D}(\boldsymbol{s})\exp\{\mathrm{i}k(n(\boldsymbol{s})\boldsymbol{s}\cdot\boldsymbol{r}-ct)\}],\quad \text{and similarly for } \boldsymbol{B},\ \boldsymbol{E},\ \boldsymbol{H}. \tag{2.1}$$

Here $n(\boldsymbol{s})$ is the refractive index, and $\boldsymbol{D}(\boldsymbol{s})$, etc., are the complex polarization states of the three-dimensional field vectors, that is

$$\boldsymbol{D}(\boldsymbol{s})=\{D_1(\boldsymbol{s}),D_2(\boldsymbol{s}),D_3(\boldsymbol{s})\},\mathrm{etc.},\quad \text{where } \boldsymbol{s}=\{s_1,s_2,s_3\},\quad \boldsymbol{s}\cdot\boldsymbol{s}=1. \tag{2.2}$$

As in Berry & Dennis (2003), it is convenient to write the constitutive relations in terms of reciprocal dielectric and magnetic permeability tensors relative to a vacuum, that is, to express $\boldsymbol{E}$ and $\boldsymbol{H}$ in terms of $\boldsymbol{D}$ and $\boldsymbol{B}$, rather than the reverse as is customary; thus

$$\begin{pmatrix}\boldsymbol{E}\\ \boldsymbol{H}\end{pmatrix}=\begin{pmatrix}\dfrac{\boldsymbol{\eta}_{\mathrm{e}}^{(3)}}{\varepsilon_0} & \dfrac{\boldsymbol{\eta}_{\mathrm{em}}^{(3)}}{\sqrt{\varepsilon_0\mu_0}}\\ \dfrac{\boldsymbol{\eta}_{\mathrm{me}}^{(3)}}{\sqrt{\varepsilon_0\mu_0}} & \dfrac{\boldsymbol{\eta}_{\mathrm{m}}^{(3)}}{\mu_0}\end{pmatrix}\begin{pmatrix}\boldsymbol{D}\\ \boldsymbol{B}\end{pmatrix}\equiv\mathbf{N}^{(3)}\begin{pmatrix}\boldsymbol{D}\\ \boldsymbol{B}\end{pmatrix}. \tag{2.3}$$

The 72 real components of the 6×6 complex matrix $\mathbf{N}^{(3)}$ will be regarded as constants, independent of the direction of $\boldsymbol{s}$ but possibly dependent on frequency $\omega=ck$, external static electric and magnetic fields, and temperature and stress. There will be no restriction on these constants arising from causality, because we are considering monochromatic waves at a fixed frequency, so that dispersion relations, which involve integrations over all frequencies, are irrelevant.

It is useful to characterize the four constituent 3×3 matrices in terms of the effects each would produce if acting alone. Thus, for the electric–electric matrix

and with superscripts T denoting the matrix transpose

$$\left.\begin{array}{l}\boldsymbol{\eta}_{\mathrm{e}}^{(3)}:\\ \text{symmetric part } \boldsymbol{\eta}_{\mathrm{e,s}}^{(3)}=\frac{1}{2}(\boldsymbol{\eta}_{\mathrm{e}}^{(3)}+\boldsymbol{\eta}_{\mathrm{e}}^{(3)\mathrm{T}})\\ \quad\Rightarrow\text{inverse electric permittivity tensor}\\ \quad(\mathrm{Re}\,\boldsymbol{\eta}_{\mathrm{e,s}}^{(3)}\Rightarrow\text{transparency},\quad \mathrm{Im}\,\boldsymbol{\eta}_{\mathrm{e,s}}^{(3)}\Rightarrow\text{absorption}),\\ \text{antisymmetric part } \boldsymbol{\eta}_{\mathrm{e,a}}^{(3)}=\frac{1}{2}(\boldsymbol{\eta}_{\mathrm{e}}^{(3)}-\boldsymbol{\eta}_{\mathrm{e}}^{(3)\mathrm{T}})\\ \quad\Rightarrow\text{Faraday rotation}\\ \quad(\mathrm{Im}\,\boldsymbol{\eta}_{\mathrm{e,a}}^{(3)}\Rightarrow\text{transparency},\quad \mathrm{Re}\,\boldsymbol{\eta}_{\mathrm{e,a}}^{(3)}\Rightarrow\text{absorption}),\end{array}\right\}\tag{2.4}$$

where the interpretation of the antisymmetric part as Faraday rotation envisages these matrix components as dependent on static external fields. For the corresponding magnetic–magnetic matrix

$$\left.\begin{array}{l}\boldsymbol{\eta}_{\mathrm{m}}^{(3)}:\\ \text{symmetric part } \boldsymbol{\eta}_{\mathrm{m,s}}^{(3)}=\frac{1}{2}(\boldsymbol{\eta}_{\mathrm{m}}^{(3)}+\boldsymbol{\eta}_{\mathrm{m}}^{(3)\mathrm{T}})\\ \quad\Rightarrow\text{inverse magnetic permeability tensor}\\ \quad(\mathrm{Re}\,\boldsymbol{\eta}_{\mathrm{m,s}}^{(3)}\Rightarrow\text{transparency},\quad \mathrm{Im}\,\boldsymbol{\eta}_{\mathrm{m,s}}^{(3)}\Rightarrow\text{absorption}),\\ \text{antisymmetric part } \boldsymbol{\eta}_{\mathrm{m,a}}^{(3)}=\frac{1}{2}(\boldsymbol{\eta}_{\mathrm{m}}^{(3)}-\boldsymbol{\eta}_{\mathrm{m}}^{(3)\mathrm{T}})\\ \quad\Rightarrow\text{dual Faraday rotation}\\ \quad(\mathrm{Im}\,\boldsymbol{\eta}_{\mathrm{m,a}}^{(3)}\Rightarrow\text{transparency},\quad \mathrm{Re}\,\boldsymbol{\eta}_{\mathrm{m,a}}^{(3)}\Rightarrow\text{absorption}),\end{array}\right\}\tag{2.5}$$

where the term 'dual Faraday rotation' refers to the coupling of external fields to the magnetic field of the plane wave.

For the matrices coupling the electric and magnetic fields

$$\left.\begin{array}{l}\boldsymbol{\eta}_{\mathrm{em}}^{(3)}\quad\text{and}\quad\boldsymbol{\eta}_{\mathrm{me}}^{(3)}:\\ \text{antisymmetric combination } \boldsymbol{\eta}_{\mathrm{cross,a}}^{(3)}=\frac{1}{2}(\boldsymbol{\eta}_{\mathrm{me}}^{(3)}-\boldsymbol{\eta}_{\mathrm{em}}^{(3)\mathrm{T}})\\ \quad\Rightarrow\text{natural optical activity tensor}\\ \quad(\mathrm{Im}\,\boldsymbol{\eta}_{\mathrm{cross,a}}^{(3)}\Rightarrow\text{transparency},\quad \mathrm{Re}\,\boldsymbol{\eta}_{\mathrm{cross,a}}^{(3)}\Rightarrow\text{absorption}),\\ \text{symmetric combination } \boldsymbol{\eta}_{\mathrm{cross,s}}^{(3)}=\frac{1}{2}(\boldsymbol{\eta}_{\mathrm{em}}^{(3)}+\boldsymbol{\eta}_{\mathrm{me}}^{(3)\mathrm{T}})\\ \quad\Rightarrow\text{bianisotropy tensor}\\ \quad(\mathrm{Re}\,\boldsymbol{\eta}_{\mathrm{cross,s}}^{(3)}\Rightarrow\text{transparency},\quad \mathrm{Im}\,\boldsymbol{\eta}_{\mathrm{cross,s}}^{(3)}\Rightarrow\text{absorption}).\end{array}\right\}\tag{2.6}$$

Here, the interpretation of the antisymmetric combination as natural optical activity is based on the representation of this effect as a coupling between the field $\boldsymbol{E}_{\mathrm{phys}}$ (or $\boldsymbol{H}_{\mathrm{phys}}$) with the rate of change $\mathrm{d}\boldsymbol{B}_{\mathrm{phys}}/\mathrm{d}t$ (or $\mathrm{d}\boldsymbol{D}_{\mathrm{phys}}/\mathrm{d}t$, rather than the alternative coupling of $\boldsymbol{E}_{\mathrm{phys}}$ (or $\boldsymbol{H}_{\mathrm{phys}}$) with $\boldsymbol{\nabla}\times\boldsymbol{E}_{\mathrm{phys}}$ (or $\boldsymbol{\nabla}\times\boldsymbol{H}_{\mathrm{phys}}$), which would involve the direction $\boldsymbol{s}$ of the wave (because of Maxwell's equations in the frequency domain, the two descriptions are essentially

equivalent). True bianisotropic coupling is represented by the symmetric combination.

The interpretations (2.4)–(2.6) imply that for a transparent crystal, that is, a crystal without absorption, the 6×6 matrix in (2.3) is Hermitian, that is $\mathbf{N}^{(3)}=\mathbf{N}^{(3)\dagger}$; this case will be explored in §6*a*.

Two observations enable the dimension of the parameter space of bianisotropic crystals to be reduced. Coordinate axes can be rotated to make the symmetric part of $\mathrm{Re}\,\boldsymbol{\eta}_{\mathrm{e}}^{(3)}$ diagonal (its three components are then the reciprocals of the principal dielectric constants); this eliminates three real parameters. And since $\mathrm{tr}\,\boldsymbol{\eta}_{\mathrm{e}}^{(3)}$ and $\mathrm{tr}\,\boldsymbol{\eta}_{\mathrm{m}}^{(3)}$ represent trivial isotropic refraction and absorption, which can be easily eliminated, only the traceless part of these two matrices needs be included in the count of parameters influencing the polarization states; this eliminates one complex parameter from each of the two matrices, that is, four real parameters in all. The remaining number of parameters is $72-3-4=65$.

Further reduction, based on symmetries not considered here appropriate to particular crystal classes, might be possible. We have also not incorporated the 'Post constraint', namely

$$\mathrm{tr}[\boldsymbol{\eta}_{\mathrm{e}}^{-1}(\boldsymbol{\eta}_{\mathrm{em}}+\boldsymbol{\eta}_{\mathrm{me}})]=0, \tag{2.7}$$

(see Lakhtakia 2004; Raab & de Lange 2005), whose universal applicability is the subject of controversy (Hehl & Obukhov 2004); although this complex condition would reduce the number of parameters by two, it imposes no restriction on the singularities we are considering here.

3. 4×4 Stereographic formulation

For the plane waves (2.1), Maxwell's equations reduce to

$$\frac{1}{n(\boldsymbol{s})}\begin{pmatrix}\boldsymbol{D}(\boldsymbol{s})\\ \boldsymbol{B}(\boldsymbol{s})\end{pmatrix}=\frac{1}{c}\begin{pmatrix}-\boldsymbol{s}\times\boldsymbol{H}(\boldsymbol{s})\\ \boldsymbol{s}\times\boldsymbol{E}(\boldsymbol{s})\end{pmatrix}. \tag{3.1}$$

A convenient explicit representation of the sphere of directions $\boldsymbol{s}$, eliminating the singularity at the north pole introduced by polar coordinates θ, ϕ, is a south-pole stereographic projection onto the 'plane of directions' $\boldsymbol{R}$, defined by

$$\left.\begin{aligned}\boldsymbol{R}=\{X,\,Y\}&=R(\cos\phi,\sin\phi)=\frac{\{s_x,\,s_y\}}{s_z+1}=\tan\tfrac{1}{2}\theta\,(\cos\phi,\sin\phi),\\ \boldsymbol{s}&=\frac{1}{1+R^2}\{2X,2Y,1-R^2\}.\end{aligned}\right\} \tag{3.2}$$

By (3.1), the fields $\boldsymbol{D}(\boldsymbol{s})$ and $\boldsymbol{B}(\boldsymbol{s})$ lie in the plane perpendicular to $\boldsymbol{s}$; we choose coordinates in this plane, with axes along the Cartesian directions X

and Y. Thus we define transverse fields

$$\left.\begin{aligned} \boldsymbol{d} &\equiv \frac{1}{\sqrt{\varepsilon_0}}(\mathcal{R}(\boldsymbol{R})\boldsymbol{D})_{\mathrm{trans}} = \begin{pmatrix} d_X \\ d_Y \end{pmatrix}, \quad \boldsymbol{b} \equiv \frac{1}{\sqrt{\mu_0}}(\mathcal{R}(\boldsymbol{R})\boldsymbol{B})_{\mathrm{trans}} = \begin{pmatrix} b_X \\ b_Y \end{pmatrix}, \\ \boldsymbol{e} &\equiv (\mathcal{R}(\boldsymbol{R})\boldsymbol{E})_{\mathrm{trans}} = \begin{pmatrix} e_X \\ e_Y \end{pmatrix}, \qquad \boldsymbol{h} \equiv (\mathcal{R}(\boldsymbol{R})\boldsymbol{H})_{\mathrm{trans}} = \begin{pmatrix} h_X \\ h_Y \end{pmatrix}, \end{aligned}\right\} \tag{3.3}$$

incorporating convenient scalings and the rotation matrix effecting the coordinate rotation. When calculated as a three-dimensional rotation to θ, ϕ followed by a two-dimensional rotation to X, Y, the matrix is

$$\mathcal{R}(\boldsymbol{R}) = \frac{1}{1+X^2+Y^2}\begin{pmatrix} 1-X^2+Y^2 & -2XY & -2X \\ -2XY & 1+X^2-Y^2 & -2Y \\ 2X & 2Y & 1-X^2-Y^2 \end{pmatrix}. \tag{3.4}$$

Maxwell's equations now become

$$\frac{1}{n(\boldsymbol{R})}\begin{pmatrix} \sqrt{\varepsilon_0}\boldsymbol{d}(\boldsymbol{R}) \\ \sqrt{\mu_0}\boldsymbol{b}(\boldsymbol{R}) \end{pmatrix} = \frac{1}{c}\begin{pmatrix} \mathbf{0} & \mathbf{j} \\ -\mathbf{j} & \mathbf{0} \end{pmatrix}\begin{pmatrix} \boldsymbol{e}(\boldsymbol{R}) \\ \boldsymbol{h}(\boldsymbol{R}) \end{pmatrix}, \tag{3.5}$$

where

$$\mathbf{0} = \begin{pmatrix} 0 & 0 \\ 0 & 0 \end{pmatrix} \quad \text{and} \quad \mathbf{j} = \begin{pmatrix} 0 & 1 \\ -1 & 0 \end{pmatrix}, \quad \text{i.e. } \mathbf{j}^2 = -\mathbf{1}. \tag{3.6}$$

Incorporating the constitutive relations (2.3) gives

$$\frac{1}{n(\boldsymbol{R})}\begin{pmatrix} \boldsymbol{d}(\boldsymbol{R}) \\ \boldsymbol{b}(\boldsymbol{R}) \end{pmatrix} = \mathbf{M}(\boldsymbol{R})\begin{pmatrix} \boldsymbol{d}(\boldsymbol{R}) \\ \boldsymbol{b}(\boldsymbol{R}) \end{pmatrix}, \tag{3.7}$$

where the 4×4 matrix $\mathbf{M}$ is

$$\begin{aligned} \mathbf{M}(\boldsymbol{R}) &= \frac{1}{c}\begin{pmatrix} \mathbf{0} & \mathbf{j} \\ -\mathbf{j} & \mathbf{0} \end{pmatrix}\begin{pmatrix} \boldsymbol{\eta}_{\mathrm{e}}(\boldsymbol{R}) & \boldsymbol{\eta}_{\mathrm{em}}(\boldsymbol{R}) \\ \boldsymbol{\eta}_{\mathrm{me}}(\boldsymbol{R}) & \boldsymbol{\eta}_{\mathrm{m}}(\boldsymbol{R}) \end{pmatrix} \\ &\equiv \begin{pmatrix} \mathbf{0} & \mathbf{j} \\ -\mathbf{j} & \mathbf{0} \end{pmatrix}\mathbf{N}(\boldsymbol{R}) = \frac{1}{c}\begin{pmatrix} \mathbf{j}\boldsymbol{\eta}_{\mathrm{me}}(\boldsymbol{R}) & \mathbf{j}\boldsymbol{\eta}_{\mathrm{m}}(\boldsymbol{R}) \\ -\mathbf{j}\boldsymbol{\eta}_{\mathrm{e}}(\boldsymbol{R}) & -\mathbf{j}\boldsymbol{\eta}_{\mathrm{em}}(\boldsymbol{R}) \end{pmatrix}, \end{aligned} \tag{3.8}$$

in which the constituent 2×2 matrices are

$$\boldsymbol{\eta}_{\mathrm{e}}(\boldsymbol{R}) = (\mathcal{R}(\boldsymbol{R})\boldsymbol{\eta}_{\mathrm{e}}^{(3)}\mathcal{R}^{-1}(\boldsymbol{R}))_{\mathrm{trans}}, \text{ etc.} \tag{3.9}$$

In Berry & Dennis (2003) a further transformation is employed, to the right- and left-circularly polarized components of $\boldsymbol{d}$, but this will be avoided here.

It is easily confirmed that the 2×2 matrices, $\boldsymbol{\eta}_{\mathrm{e}}(\boldsymbol{R})$, etc., in (3.9), inherit the symmetries (2.4)–(2.6) of their generating 3×3 matrices, $\boldsymbol{\eta}_{\mathrm{e}}^{(3)}$, etc.

The equations (3.7) form a 4×4 eigensystem, whose eigenvalues give four (generally complex) refractive indices $n^{(i)}(\boldsymbol{R})$. Corresponding to each are the

eigenpolarizations, namely the complex 2-vectors $\boldsymbol{d}^{(i)}(\boldsymbol{R})$ and $\boldsymbol{b}^{(i)}(\boldsymbol{R})$. Where no confusion will result, the superscripts (i) and the $\boldsymbol{R}$ dependence will be omitted. It will be convenient to represent these polarization vectors in a way that is independent of normalization and overall phase, by the ratios of their components, that is, by the complex numbers

$$w_{\mathrm{e}} \equiv \frac{d_Y}{d_X}, \quad w_{\mathrm{m}} \equiv \frac{b_Y}{b_X}. \tag{3.10}$$

The material in this section is a version of the standard '*kDB*' formalism (Kong 1974, 1975), with the slightly different rotation matrix corresponding to expressing the field components in stereographic, rather than polar, coordinates. For an alternative 4×4 formalism, see Tan & Tan (2000).

4. Singularities

Our emphasis here is on the singularities in the $\boldsymbol{R}$ plane that occur generically, that is, for typical choices of the crystal parameters and which are therefore stable under variations of those parameters. There are three such singularities.

First are the *degeneracies*. These are the generalizations of the 'singular axes' of dielectric anisotropy, corresponding to Voigt waves (Voigt 1902; Pancharatnam 1958; Ramachandran & Ramaseshan 1961), defined by

$$n^{(i)}(\boldsymbol{R}) = n^{(j)}(\boldsymbol{R}) \quad (i \neq j), \tag{4.1}$$

satisfying

$$\det\left[\mathbf{M} - \frac{1}{n}\mathbf{1}\right] = 0 \quad \text{and} \quad \frac{\mathrm{d}}{\mathrm{d}n}\det\left[\mathbf{M} - \frac{1}{n}\mathbf{1}\right] = 0. \tag{4.2}$$

Only pairwise degeneracies will be considered here, because these typically (that is, stably under perturbation, i.e. generically) have codimension 2 and so occur as points in direction space $\boldsymbol{s}$ or $\boldsymbol{R}$ for typical crystals.

Degeneracies involving three or four eigenvalues have higher codimension and so will not occur typically, though particular crystal symmetries might enforce them. Other special types of degeneracy occur in uniaxial bianisotropic crystals (Lakhtakia *et al.* 1991), and as generalizations of Voigt waves near interfaces (Borzdov 1990*a*,*b*, 1996) and in twisted media (Lakhtakia 1998) (these can be viewed as generalizations of critical damping in oscillation theory).

When absorption is present, the degeneracies are square-root branch-points (Berry & Dennis 2003; Berry 2004*b*), near which the separation $|n^{(i)}(\boldsymbol{R}) - n^{(j)}(\boldsymbol{R})| \propto \sqrt{\Delta}$, where Δ is the distance from the degeneracy. When there is no absorption but where chirality (natural optical activity or the Faraday effect) is present, there are typically no degeneracies. When both absorption and chirality are absent, the degeneracies are conical points, near which $|n^{(i)}(\boldsymbol{R}) - n^{(j)}(\boldsymbol{R})| \propto \Delta$.

If the indices are ordered by the magnitudes of their real parts (with the largest first), possible degeneracies are between $(i, j) = (1, 2)$, $(2, 3)$ and $(3, 4)$. However, even for large anisotropy and coupling, the eigenvalues seem to divide into a pair with Re $n > 0$ and a pair with Re $n < 0$ (see §§6*a*,*b* for situations where

this is always the case). Therefore, we consider only degeneracies between the upper two levels (1,2) or the lower two levels (3,4), and ignore (though not exclude) the possibility of degeneracies between the middle pair (2,3), since this would require Re n to cross zero as a crystal parameter is varied. Of course the degeneracies for a given eigenpolarization are common to the fields $\boldsymbol{d}$, $\boldsymbol{b}$, $\boldsymbol{e}$ and $\boldsymbol{h}$.

Second, there are the electric and magnetic *circular polarization singularities* C_{e} and C_{m}. Pure circular polarization of any of the eight 2-vectors $\boldsymbol{d}^{(i)}$ and $\boldsymbol{b}^{(i)}$ requires the two components to be equal in magnitude and differ in phase by $\pi/2$, giving the conditions

$$C_{\mathrm{e}} : w_{\mathrm{e}} = \pm\mathrm{i}, \quad \text{i.e. } w_{\mathrm{e}}^2 = -1; \quad C_{\mathrm{m}} : w_{\mathrm{m}} = \pm\mathrm{i}, \quad \text{i.e. } w_{\mathrm{m}}^2 = -1. \tag{4.3}$$

The solution of any of these complex scalar equations requires two conditions, so the C_{e} and C_{m} singularities are typically points in the $\boldsymbol{R}$ plane.

As will become clear later, the C_{e} and C_{m} singularities for all four polarizations typically occur in different directions. There are, however, special crystals and particular directions where all eigenwaves are circularly polarized for both the $\boldsymbol{d}$ and $\boldsymbol{b}$ fields (Lakhtakia 2001, 2002). These are interesting physically, and also mathematically (because of the connection to Beltrami fields), but do not fall into the class being considered here because they are not stable under perturbation and so are not typical.

Third, there are the electric and magnetic *linear polarization singularities* L_{e} and L_{m}. Pure linear polarization of any of the eight 2-vectors $\boldsymbol{d}^{(i)}$ and $\boldsymbol{b}^{(i)}$ requires the phases of the two components to be the same or to differ by π, i.e. w is real, giving the conditions

$$L_{\mathrm{e}} : \mathrm{Im}\, w_{\mathrm{e}} = 0; \quad L_{\mathrm{m}} : \mathrm{Im}\, w_{\mathrm{m}} = 0. \tag{4.4}$$

These are real scalar equations, so the L_{e} and L_{m} singularities are typically lines in the $\boldsymbol{R}$ plane.

For a given eigenpolarization, the vectors $\boldsymbol{d}$ and $\boldsymbol{b}$ are different, so the electric singularities C_{e} and L_{e} do not coincide with their magnetic counterparts C_{m} and L_{m}. What about the C and L singularities of the fields $\boldsymbol{e}$ and $\boldsymbol{h}$? These do not need to be considered separately, since the Maxwell equations (3.5) imply

$$w(\boldsymbol{d}\,\text{field}) = -\frac{1}{w(\boldsymbol{h}\,\text{field})}, \quad w(\boldsymbol{b}\,\text{field}) = -\frac{1}{w(\boldsymbol{e}\,\text{field})}, \tag{4.5}$$

and it follows from (4.3) and (4.4) that the C and L singularities of $\boldsymbol{d}$ coincide with those of $\boldsymbol{h}$, and the C and L singularities of $\boldsymbol{b}$ coincide with those of $\boldsymbol{e}$. (We note a potential confusion arising from this interlacing of singularities, arising from the otherwise-convenient choices of the suffix 'e' to describe aspects of the $\boldsymbol{d}$ field, whose C and L singularities are shared by $\boldsymbol{h}$, and the suffix 'm' to describe aspects of the $\boldsymbol{b}$ field, whose C and L singularities are shared by $\boldsymbol{e}$. This simply reflects the fundamental interplay of electricity and magnetism embodied in Maxwell's equations.)

5. Numerics

To illustrate some of the singularities displayed by bianisotropic crystals, we reduce the 65-dimensional crystal space (§2) to a six-dimensional subspace based on the following constitutive matrices:

$$\left.\begin{aligned}
\boldsymbol{\eta}_{\mathrm{e}}^{(3)} &= \mathbf{1} + a_{\mathrm{e}}(\boldsymbol{\Delta}_{\mathrm{ea}}^{(3)} + \mathrm{i}d\boldsymbol{\Delta}_{\mathrm{ead}}^{(3)}) + \mathrm{i}f(\boldsymbol{\eta}_{\mathrm{ef}}^{(3)} + \mathrm{i}d\boldsymbol{\eta}_{\mathrm{efd}}^{(3)}),\\
\boldsymbol{\eta}_{\mathrm{m}}^{(3)} &= \mathbf{1} + a_{\mathrm{m}}(\boldsymbol{\Delta}_{\mathrm{ma}}^{(3)} + \mathrm{i}d\boldsymbol{\Delta}_{\mathrm{mad}}^{(3)}) + \mathrm{i}f(\boldsymbol{\eta}_{\mathrm{mf}}^{(3)} + \mathrm{i}d\boldsymbol{\eta}_{\mathrm{mfd}}^{(3)}),\\
\boldsymbol{\eta}_{\mathrm{em}}^{(3)} &= \mathrm{i}c(\boldsymbol{\eta}_{\mathrm{emc}}^{(3)} + \mathrm{i}d\boldsymbol{\eta}_{\mathrm{emcd}}^{(3)}) + b(\boldsymbol{\eta}_{\mathrm{emb}}^{(3)} + \mathrm{i}d\boldsymbol{\eta}_{\mathrm{embd}}^{(3)}),\\
\boldsymbol{\eta}_{\mathrm{me}}^{(3)} &= -\mathrm{i}c(\boldsymbol{\eta}_{\mathrm{emc}}^{(3)\mathrm{T}} + \mathrm{i}d\boldsymbol{\eta}_{\mathrm{emcd}}^{(3)\mathrm{T}}) + b(\boldsymbol{\eta}_{\mathrm{emb}}^{(3)\mathrm{T}} + \mathrm{i}d\boldsymbol{\eta}_{\mathrm{embd}}^{(3)\mathrm{T}}).
\end{aligned}\right\} \tag{5.1}$$

In $\boldsymbol{\eta}_{\mathrm{e}}^{(3)}$ and $\boldsymbol{\eta}_{\mathrm{m}}^{(3)}$, the unit matrices $\mathbf{1}$ represent isotropic crystals; in reality, $\mathrm{tr}\,\boldsymbol{\eta}_{\mathrm{e}}^{(3)}$ and $\mathrm{tr}\,\boldsymbol{\eta}_{\mathrm{m}}^{(3)}$ can be arbitrary complex constants, but these can be eliminated by elementary rescaling of the fields and matrices. The parameters (real numbers) are

$$p = \{a_{\mathrm{e}}, a_{\mathrm{m}}, d, c, b, f\}, \tag{5.2}$$

with the following interpretations, derived from (2.4) to (2.6)

$$\left.\begin{aligned}
&a_{\mathrm{e}}: \text{electric anisotropy}; \quad a_{\mathrm{m}}: \text{magnetic anisotropy};\\
&d: \text{dissipation}; \quad c: \text{chirality (natural optical activity)};\\
&b: \text{bianisotropy}; \quad f: \text{Faraday effect}.
\end{aligned}\right\} \tag{5.3}$$

The $\boldsymbol{\Delta}_{\mathrm{ea}}^{(3)}$, etc., are 3×3 matrices whose elements are random real numbers, chosen as explained in appendix A and listed there. This family of crystals can be guaranteed to be absorbing in all directions (the imaginary parts of all refractive indices are positive for all $\boldsymbol{s}$), rather than active (imaginary parts negative), by exploiting the trace freedom already mentioned and choosing $\mathrm{Im}\,\mathrm{tr}\,\boldsymbol{\eta}_{\mathrm{e}}^{(3)}$ and $\mathrm{Im}\,\mathrm{tr}\,\boldsymbol{\eta}_{\mathrm{m}}^{(3)}$ sufficiently large and positive.

The six-dimensional p space is still too large for comprehensive exploration. Instead, we will present a series of pictures illustrating the deportment of the singularities. The common conventions employed in these pictures are as follows.

Each picture represents a region of direction space $\boldsymbol{R}$, coloured by hue, encoding the phase of the ratio of the components of $\boldsymbol{d}$ or $\boldsymbol{b}$ on the basis of circular polarization states, that is,

$$\arg w_{\mathrm{e}}^{(\mathrm{circular})} \quad \text{or} \quad \arg w_{\mathrm{m}}^{(\mathrm{circular})},$$

where

$$\left.\begin{aligned}
w_{\mathrm{e}}^{(\mathrm{circular})} &\equiv \frac{d_{\text{left-handed}}}{d_{\text{right-handed}}} = \frac{1+\mathrm{i}w_{\mathrm{e}}}{1-\mathrm{i}w_{\mathrm{e}}};\\
w_{\mathrm{m}}^{(\mathrm{circular})} &\equiv \frac{b_{\text{left-handed}}}{b_{\text{right-handed}}} = \frac{1+\mathrm{i}w_{\mathrm{m}}}{1-\mathrm{i}w_{\mathrm{m}}}
\end{aligned}\right\} \tag{5.4}$$

(cf. Berry & Dennis 2003). The phases are convenient because each represents twice the angle made with the X-axis by the principal axis of the polarization ellipse for the field ($\boldsymbol{d}$ or $\boldsymbol{b}$) being considered, so contours of colour are contours of polarization ellipse orientation.

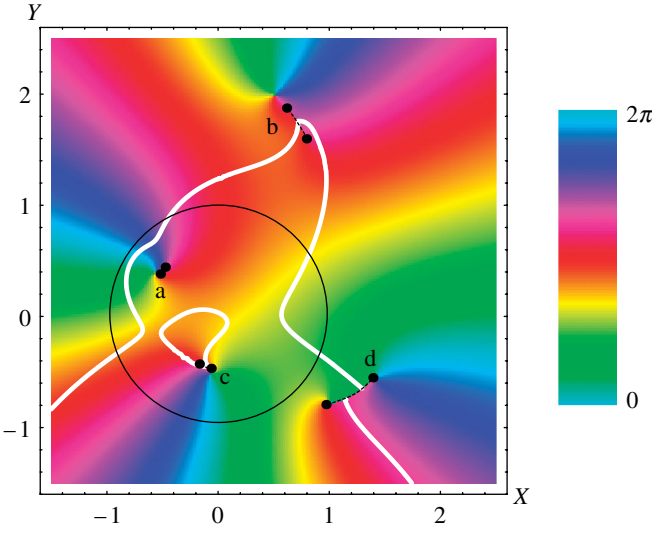

Figure 1. Polarization pattern, in direction space $\boldsymbol{R}$, of the upper electric state $\boldsymbol{d}^{(1)}$ for the typical bianisotropic absorbing chiral crystal with parameters (equation (5.2)) $p=\{0.1, 0.2, 0.3, 0.1, 0.15, 0.05\}$, depicted according to the conventions in the paragraphs following (5.3). The thin black circle encloses the 'northern hemisphere' $X^2+Y^2<1$, and the bar on the right shows the colour coding for phase.

The C points, where the orientation is undefined, are immediately evident as places where all colours meet. Degeneracies are indicated by black dots, connected in pairs by dashed lines representing branch cuts where relevant. The L lines are represented by white lines.

Figure 1 shows the polarization structure in a typical case, where all parameters p are non-zero. There are eight degeneracies, connected by branch cuts. The magnifications in figure 2 show the structure more clearly. Each degeneracy is a square-root branch point, as discussed earlier and as illustrated in figure 3. The L lines are discontinuous across the branch cuts (figure 2), but are continuous on the full Riemann surface consisting of the two connected states (e.g. $\boldsymbol{d}^{(1)}$ and $\boldsymbol{d}^{(2)}$), as shown in the magnifications in figure 4. For each of the two degenerating states, the L_{e} and L_{m} lines are close together but do not coincide. Also, as is clear from the further magnifications in figure 5, the C_{e} and C_{m} points do not coincide. And although we do not show this, the C_{e} points do not coincide for the two near-degenerating states $\boldsymbol{d}^{(1)}$ and $\boldsymbol{d}^{(2)}$, nor the C_{m} points for $\boldsymbol{b}^{(1)}$ and $\boldsymbol{b}^{(2)}$.

6. Special cases

(a) *Transparent crystals*

As previously stated, the condition for transparency is that the 6×6 matrix $\mathbf{N}^{(3)}$ is Hermitian

$$\mathbf{N}^{(3)}=\mathbf{N}^{(3)\dagger},\quad \text{i.e. } \boldsymbol{\eta}_{\mathrm{e}}^{(3)}=\boldsymbol{\eta}_{\mathrm{e}}^{(3)\dagger},\quad \boldsymbol{\eta}_{\mathrm{m}}^{(3)}=\boldsymbol{\eta}_{\mathrm{m}}^{(3)\dagger},\quad \boldsymbol{\eta}_{\mathrm{me}}^{(3)}=\boldsymbol{\eta}_{\mathrm{em}}^{(3)\dagger}. \tag{6.1}$$

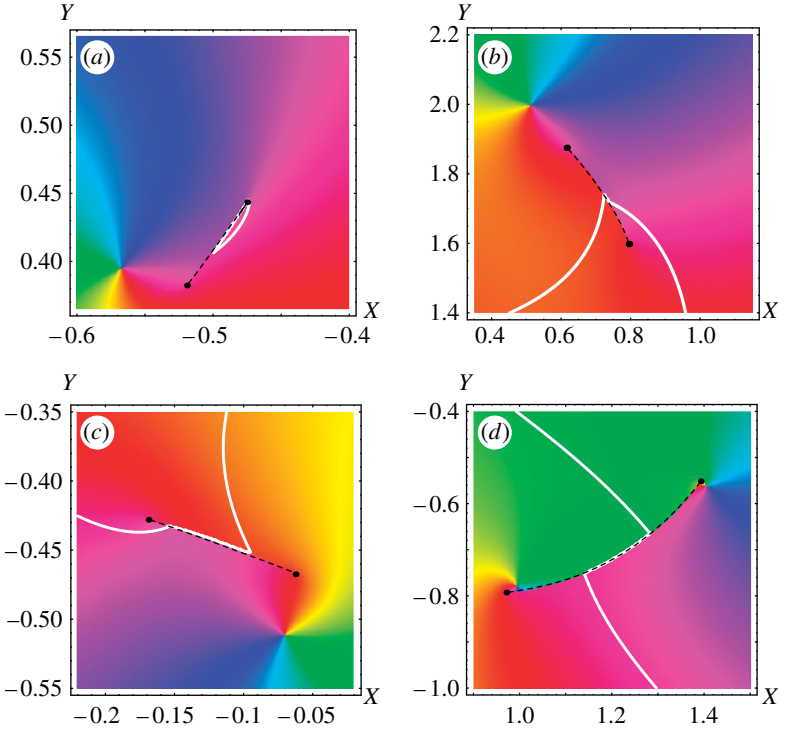

Figure 2. Magnifications of the pairs of degenerate states indicated in figure 1. (*a*) 20×; (*b*) 5×; (*c*) 20×; (*d*) 6.7×.

This well-known result (Kong 1975) follows from the requirement that no energy flows out of any fixed volume, so that the time-averaged Poynting vector is divergenceless.

By itself, equation (6.1) does not guarantee that the refractive indices are real; this requires $\mathbf{N}^{(3)}$ to be positive-definite as well as Hermitian. To see why, consider the 4×4 formalism (3.7), involving $\mathbf{M}$ defined by (3.8) and (3.9), under the transformation

$$\begin{pmatrix} \boldsymbol{d}'(\boldsymbol{r}) \\ \boldsymbol{b}'(\boldsymbol{r}) \end{pmatrix} \equiv \mathbf{N}^{1/2}(\boldsymbol{R}) \begin{pmatrix} \boldsymbol{d}(\boldsymbol{r}) \\ \boldsymbol{b}(\boldsymbol{r}) \end{pmatrix}. \tag{6.2}$$

This brings (3.7) to the form

$$\frac{1}{n(\boldsymbol{R})} \begin{pmatrix} \boldsymbol{d}'(\boldsymbol{R}) \\ \boldsymbol{b}'(\boldsymbol{R}) \end{pmatrix} = \mathbf{N}^{1/2}(\boldsymbol{R}) \begin{pmatrix} 0 & \mathbf{j} \\ -\mathbf{j} & 0 \end{pmatrix} \mathbf{N}^{1/2}(\boldsymbol{R}) \begin{pmatrix} \boldsymbol{d}'(\boldsymbol{R}) \\ \boldsymbol{b}'(\boldsymbol{R}) \end{pmatrix} \equiv \mathbf{M}'(\boldsymbol{R}) \begin{pmatrix} \boldsymbol{d}'(\boldsymbol{R}) \\ \boldsymbol{b}'(\boldsymbol{R}) \end{pmatrix}, \tag{6.3}$$

involving $\mathbf{M}'$ which is manifestly Hermitian if $\mathbf{N}^{1/2}$ is Hermitian, since the 4×4 matrix involving $\mathbf{j}$ is real symmetric. Hermiticity of $\mathbf{N}^{1/2}$ follows from that of $\mathbf{N}$, provided $\mathbf{N}$ is positive-definite. Henceforth we assume this to be true. Note that an example where $\mathbf{N}$ is not positive-definite is an isotropic crystal whose electric

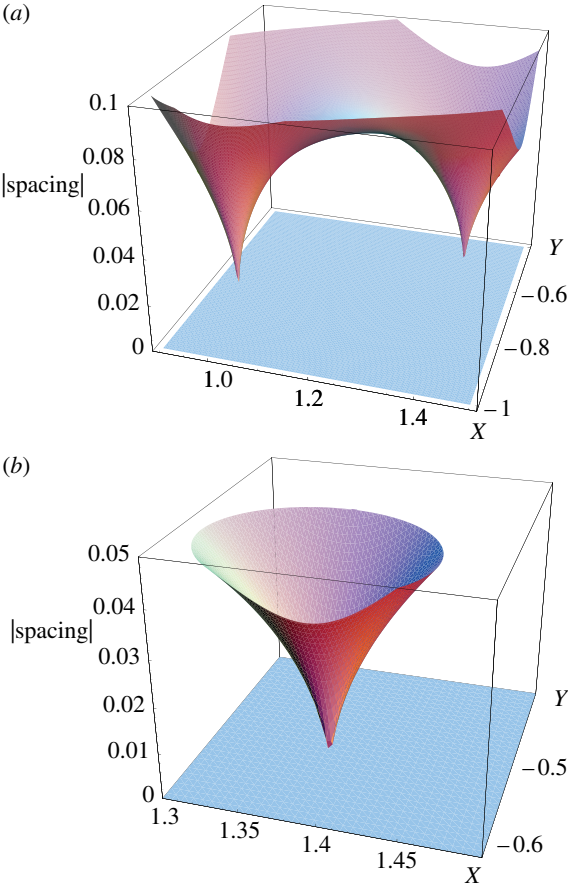

Figure 3. (a) Separation $|n^{(1)}(\boldsymbol{R})-n^{(2)}(\boldsymbol{R})|$ of the two upper $\boldsymbol{d}$ states in a region including the pair of degeneracies labelled 'd' in figure 1; (b) magnification of (a), showing the square-root structure of the degeneracy.

permittivity and magnetic permeability have opposite signs (this can occur in metals below the plasma frequency), leading to evanescent waves; such situations are irrelevant to the singularities of interest here.

The existence of four refractive indices, and the associated four polarization states, might appear incompatible with the existence of only two polarizations for a transparent crystal. But it is not hard to show that two of the indices are always positive and two are always negative (the argument involves continuation from the situation where the rotated constitutive matrix $\mathbf{N}(\boldsymbol{R})$ in (3.8) is diagonal). Since the replacement $n\rightarrow -n$ is equivalent to $\boldsymbol{s}\rightarrow -\boldsymbol{s}$, the negative n values correspond to waves travelling not along $\boldsymbol{s}$ but along $-\boldsymbol{s}$, removing the contradiction. There is no implication that the positive and negative values are equal in magnitude, as in the special case studied in §6*b*.

Figure 6 illustrates the singularity structure of a typical transparent crystal, where the parameter $d=0$ in (5.3). There are C and L singularities but no degeneracies. This is because in the presence of chirality the matrix $\mathbf{M}'(\boldsymbol{R})$ is complex Hermitian, and for such matrices degeneracies have codimension 3

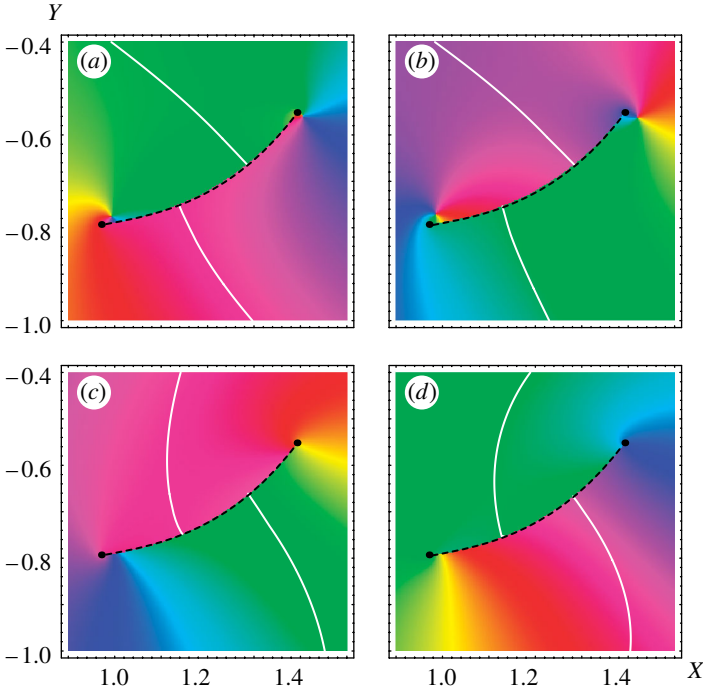

Figure 4. (*a*) Magnification (6.7×) of region of $\boldsymbol{d}^{(1)}$ pattern including the pair of degeneracies labelled 'd' in figure 1 (this is the same as figure 2*d*); (*b*) as (*a*), for the corresponding magnetic state $\boldsymbol{b}^{(1)}$; (*c*) as (*a*), for the other state $\boldsymbol{d}^{(2)}$ of the degenerating pair; (*d*) as (*c*), for $\boldsymbol{b}^{(2)}$.

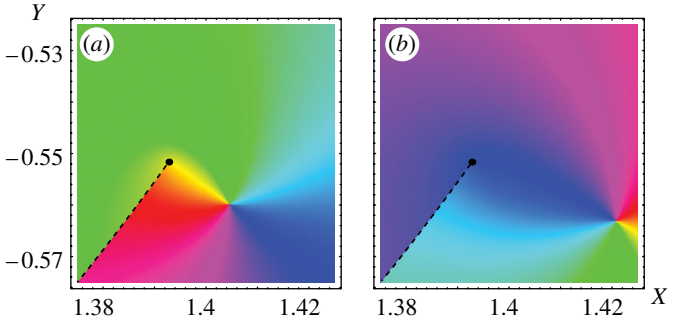

Figure 5. (*a*) Magnification (12×) of figure 4*a* near the right-hand degeneracy; (*b*) magnification of figure 4*b* near the right-hand degeneracy, showing separation of C points from the degeneracy and separation of C_{e} and C_{m}.

(Von Neumann & Wigner 1929), so in the two-dimensional direction space $\boldsymbol{R}$ there are typically no degeneracies. This is illustrated in figure 7: the two square-root degeneracies of figure 3*a* have condensed into a blunted cone that never reaches zero spacing. The magnifications in figure 8 indicate that all four C points, associated with the two states with Re $n>0$, are distinct.

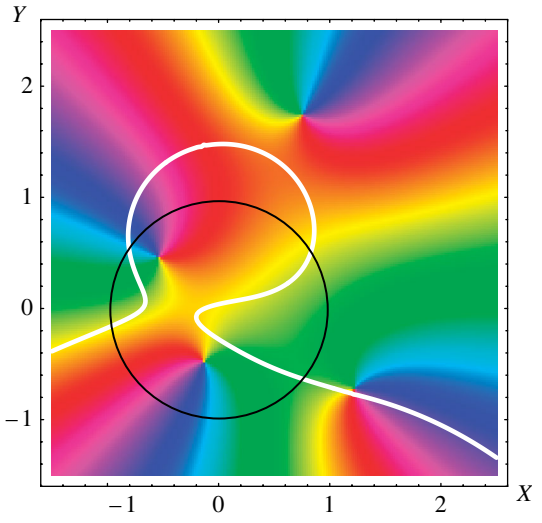

Figure 6. As figure 1, but for the transparent chiral bianisotropic crystal with $p=\{0.1, 0.2, 0, 0.1, 0.15, 0.05\}$.

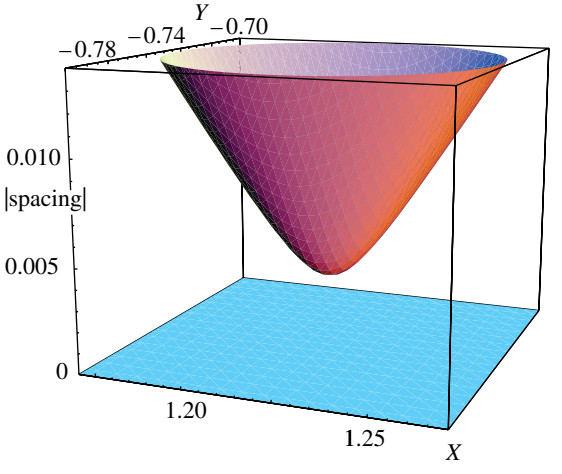

Figure 7. As figure 3, but for the transparent chiral crystal of figure 5, illustrating the absence of degeneracies.

If the crystal is transparent and non-chiral, that is, if the parameters $d=c=f=0$, the singularity structure is as illustrated in figure 9. The C point structure closely resembles the chiral case (cf. figure 5) but since $\mathbf{M}'(\boldsymbol{R})$ is now a real symmetric matrix the states $\boldsymbol{d}$, $\boldsymbol{b}$ are real and hence linearly polarized, so there are no L lines, and there are conical-point degeneracies (figure 10) rather than the near-degeneracies of the chiral case.

(*b*) *Even spectra and Lorentz reciprocity*

A common situation is for the four refractive indices n, that is, the eigenvalues of $\mathbf{M}(\boldsymbol{R})$ in (3.7), to occur in pairs $\pm n$ with opposite signs, that is $n^{(4)}=-n^{(1)}$

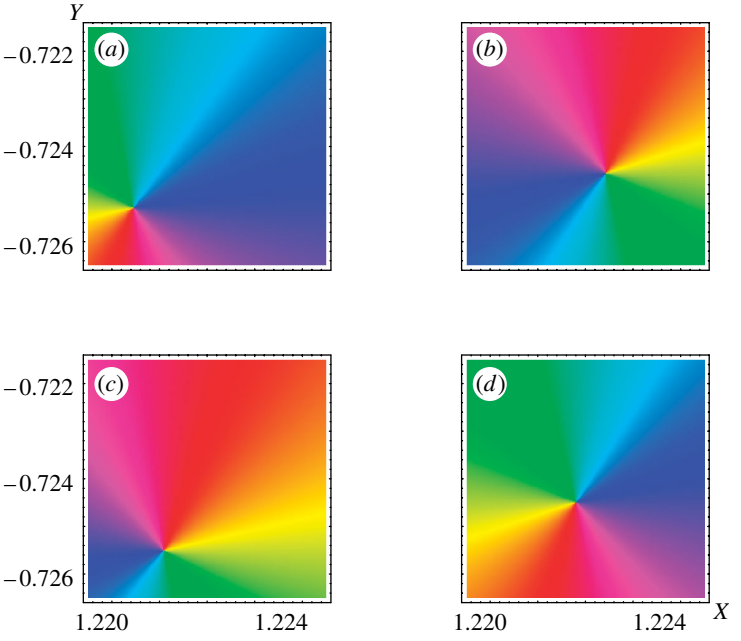

Figure 8. An 80× magnification of the right-most singularity in figure 6, for (*a*) $\boldsymbol{d}^{(1)}$, (*b*) $\boldsymbol{b}^{(1)}$, (*c*) $\boldsymbol{d}^{(2)}$ and (*d*) $\boldsymbol{b}^{(2)}$, showing that all four *C* points are distinct.

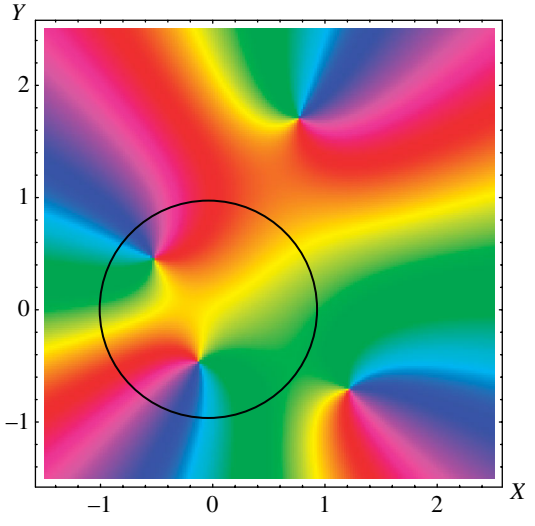

Figure 9. As figure 6, but for the transparent non-chiral bianisotropic crystal with $p=\{0.1, 0.2, 0, 0, 0.15, 0\}$; there are no *L* lines (all states are linearly polarized), and the *C* points coincide with the degeneracies.

and $n^{(3)}=-n^{(2)}$. This does not require transparency: it can happen also in absorbing crystals, for which n is complex. From (3.1), replacing n by $-n$ is equivalent to replacing $\boldsymbol{s}$ by $-\boldsymbol{s}$, so such crystals are reciprocal in the sense that waves travel in antipodal directions with the same speed (determined by Re n).

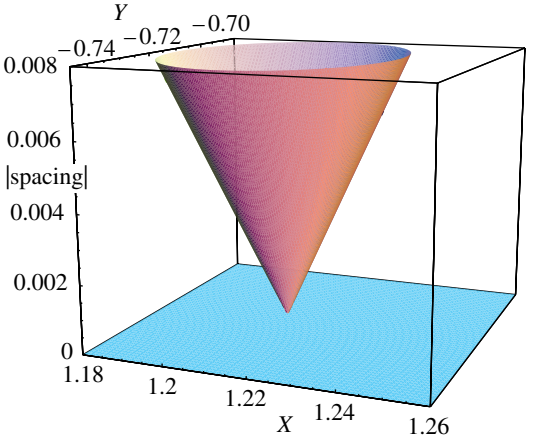

Figure 10. As figure 7, showing the conical degeneracy resulting from the coalescence of the two square-root degeneracies of figure 3*a*.

The result discussed in §6*a*, that for transparent crystals two of the (real) indices are positive and two are negative, is not a special case of this, because in that case the positive indices need not have the same magnitudes as the negative ones—that is, transparent crystals need not be reciprocal.

For the spectrum of the 4×4 matrix $\mathbf{M}(\boldsymbol{R})$ to be even in the sense just described, the characteristic polynomial $\det(\mathbf{M}-\mathbf{1}/n)$ must be even in n, which in turn requires

$$\operatorname{tr}\mathbf{M}(\boldsymbol{R}) = \operatorname{tr}\mathbf{M}^3(\boldsymbol{R}) = 0. \tag{6.4}$$

A well known and physically natural situation in which this condition is satisfied is Lorentz reciprocity (Kong 1975; Krowne 1984): crystals with electric and magnetic anisotropy and natural optical activity but no Faraday effect or bianisotropic coupling, for which (2.4)–(2.6) imply

$$\boldsymbol{\eta}_{\mathrm{e}}^{(3)} = \boldsymbol{\eta}_{\mathrm{e}}^{(3)\mathrm{T}}, \quad \boldsymbol{\eta}_{\mathrm{m}}^{(3)} = \boldsymbol{\eta}_{\mathrm{m}}^{(3)\mathrm{T}}, \quad \boldsymbol{\eta}_{\mathrm{em}}^{(3)} = -\boldsymbol{\eta}_{\mathrm{me}}^{(3)\mathrm{T}}, \tag{6.5}$$

and some algebra confirms that (6.4) holds. Lorentz reciprocity can be implemented numerically by choosing the parameters $b=f=0$ in (5.3).

(*c*) *Doubly anisotropic crystals*

Another situation for which the spectrum is even, i.e. (6.4) holds, but where (6.5) need not hold, is that of crystals for which

$$\boldsymbol{\eta}_{\mathrm{em}}^{(3)} = \boldsymbol{\eta}_{\mathrm{me}}^{(3)} = 0, \tag{6.6}$$

that is, crystals which are non-magnetoelectric (Kong 1975). Numerically, this can be implemented with parameters $b=c=0$ in (5.3). Such crystals can possess arbitrary electric and magnetic anisotropy and Faraday effects, including absorption (cf. (2.4)–(2.6)). It is easy to reduce the 4×4 system (3.7)

and (3.8), for the pair $\boldsymbol{d}$, $\boldsymbol{b}$, to 2×2 systems for $\boldsymbol{d}$ and $\boldsymbol{b}$ individually

$$\left.\begin{aligned}\frac{1}{n^2(\boldsymbol{R})}\,\boldsymbol{d}(\boldsymbol{R}) &= -\mathbf{j}\boldsymbol{\eta}_{\mathrm{m}}(\boldsymbol{R})\mathbf{j}\boldsymbol{\eta}_{\mathrm{e}}(\boldsymbol{R})\,\boldsymbol{d}(\boldsymbol{R}) \equiv \mathbf{m}_{\mathrm{e}}(\boldsymbol{R})\,\boldsymbol{d}(\boldsymbol{R}),\\ \frac{1}{n^2(\boldsymbol{R})}\,\boldsymbol{b}(\boldsymbol{R}) &= -\mathbf{j}\boldsymbol{\eta}_{\mathrm{e}}(\boldsymbol{R})\mathbf{j}\boldsymbol{\eta}_{\mathrm{m}}(\boldsymbol{R})\,\boldsymbol{b}(\boldsymbol{R}) \equiv \mathbf{m}_{\mathrm{m}}(\boldsymbol{R})\,\boldsymbol{b}(\boldsymbol{R}),\end{aligned}\right\} \tag{6.7}$$

with the occurrence of n^2 indicating that the spectrum is even. (Such materials need not be Lorentz-reciprocal in the sense of (6.5).)

An interesting phenomenon arises when, in addition, the matrices $\boldsymbol{\eta}_{\mathrm{e}}$ and $\boldsymbol{\eta}_{\mathrm{m}}$ are complex symmetric (i.e. there is no Faraday effect), so that the 6×6 constitutive matrix $\mathbf{N}^{(3)}$ in (2.3), and the 4×4 matrix $\mathbf{N}(\boldsymbol{R})$ in (3.8) are also complex symmetric. If the two eigenstates of (6.7) are denoted + and −, the C and L singularities of $\boldsymbol{d}_+$ and $\boldsymbol{b}_-$ coincide, as do those of $\boldsymbol{d}_-$ and $\boldsymbol{b}_+$. This is because in this special case

$$\mathbf{m}_{\mathrm{m}} = -\mathbf{j}\mathbf{m}_{\mathrm{e}}^{\mathrm{T}}\mathbf{j}. \tag{6.8}$$

This implies that if $\bar{\boldsymbol{d}}_\pm$ are the left eigenvectors of $\mathbf{m}_{\mathrm{e}}$, that is the eigenvectors of $\mathbf{m}_{\mathrm{e}}^{\mathrm{T}}$, then

$$\boldsymbol{b}_\pm(\boldsymbol{R}) = -\mathbf{j}\bar{\boldsymbol{d}}_\pm(\boldsymbol{R}), \tag{6.9}$$

and biorthogonality gives

$$\boldsymbol{b}_\pm(\boldsymbol{R}) = \boldsymbol{d}_\mp(\boldsymbol{R}), \tag{6.10}$$

so the singularities must coincide as described. The coincidence phenomenon was observed in numerical experiments (not shown here) with $b=c=f=0$.

There is another peculiarity about the special case discussed in the last paragraph. In the analogous purely electric non-chiral absorbing case (Berry & Dennis 2003), the C points coincide with degeneracies, giving rise to unusual singularities (e.g. index+one-quarter). With double anisotropy this does not happen: the degeneracies and C points are separated, albeit often by a very small distance in direction space $\boldsymbol{R}$, as shown in figure 11*a* and under enormous magnification in figure 11*b*. This tiny separation requires explanation, because there is a sense in which the degenerating states of a general complex symmetric matrix are chiral (Heiss & Harney 2001). However, this sense is different in the singly and doubly anisotropic cases. For pure electric anisotropy, the eigenstates of the governing 2×2 matrix are circularly polarized in the sense that each is proportional to $\{1, \pm\mathrm{i}\}$. But for symmetric matrices with dimension greater than 2, the chirality is not a circular polarization of the degenerating $\boldsymbol{d}$ or $\boldsymbol{b}$ states but rather (Heiss & Harney 2001) a factor $\pm\mathrm{i}$ in the ratio of coefficients of the degenerating state when expanded in terms of states close to the degeneracy.

7. A 2×2 matrix approximation for weak crystals

The 4×4 formalism (§3) is exact, and not difficult to implement numerically (§5). Nevertheless, a 2×2 formalism, analogous to that available for

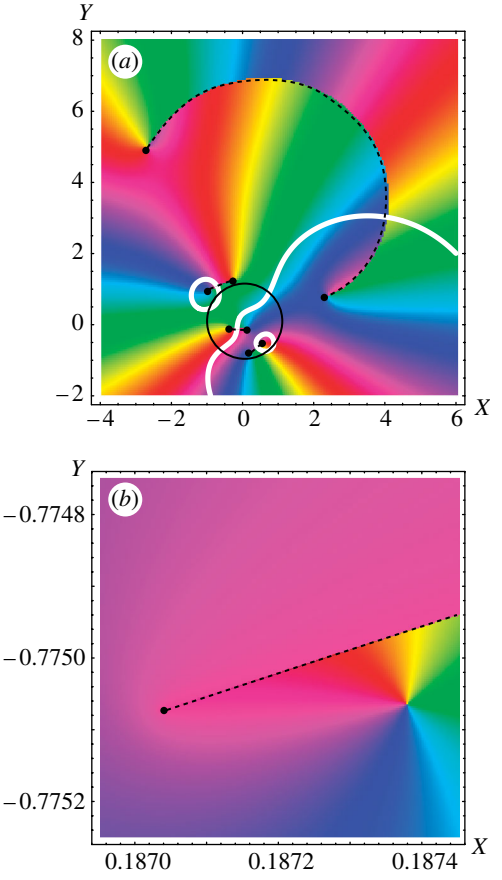

Figure 11. (*a*) As figure 1, but for the doubly anisotropic absorbing non-chiral crystal (7.14); (*b*) 20 000× magnification of the region near the lowest degeneracy in (*a*), showing separation of the C point from the degeneracy.

conventional electric anisotropy and double anisotropy (§6*c*), would be more intuitive. Such a formalism will now be derived for bianisotropic crystals that are close to isotropic but are otherwise completely general. Such 'weak crystals' are specified by

$$\boldsymbol{\eta}_{\mathrm{e}}(\boldsymbol{R}) \equiv \mathbf{1} + \boldsymbol{\Delta}_{\mathrm{e}}(\boldsymbol{R}), \quad \boldsymbol{\eta}_{\mathrm{m}}(\boldsymbol{R}) \equiv \mathbf{1} + \boldsymbol{\Delta}_{\mathrm{m}}(\boldsymbol{R}), \quad \frac{1}{n(\boldsymbol{R})} \equiv 1 + \nu(\boldsymbol{R}), \tag{7.1}$$

with

$$\|\boldsymbol{\Delta}_{\mathrm{e}}(\boldsymbol{R})\| \ll 1, \quad \|\boldsymbol{\Delta}_{\mathrm{m}}(\boldsymbol{R})\| \ll 1, \quad \|\boldsymbol{\eta}_{\mathrm{em}}(\boldsymbol{R})\| \ll 1, \quad \|\boldsymbol{\eta}_{\mathrm{me}}(\boldsymbol{R})\| \ll 1, \quad |\nu(\boldsymbol{R})| \ll 1. \tag{7.2}$$

Now we introduce the transformation (6.2) (introduced there for transparent crystals but here employed in the general case). The matrix square root in (6.2)

is, to lowest order according to (7.2)

$$\mathbf{M}'(\boldsymbol{R}) = \begin{pmatrix} \mathbf{0} & \mathbf{j} \\ -\mathbf{j} & \mathbf{0} \end{pmatrix} + \frac{1}{2}\begin{pmatrix} \boldsymbol{\Delta}_{\mathrm{e}}(\boldsymbol{R}) & \boldsymbol{\eta}_{\mathrm{em}}(\boldsymbol{R}) \\ -\boldsymbol{\eta}_{\mathrm{me}}(\boldsymbol{R}) & \boldsymbol{\Delta}_{\mathrm{m}}(\boldsymbol{R}) \end{pmatrix}\begin{pmatrix} \mathbf{0} & \mathbf{j} \\ -\mathbf{j} & \mathbf{0} \end{pmatrix} + \frac{1}{2}\begin{pmatrix} \mathbf{0} & \mathbf{j} \\ -\mathbf{j} & \mathbf{0} \end{pmatrix}\begin{pmatrix} \boldsymbol{\Delta}_{\mathrm{e}}(\boldsymbol{R}) & \boldsymbol{\eta}_{\mathrm{em}}(\boldsymbol{R}) \\ -\boldsymbol{\eta}_{\mathrm{me}}(\boldsymbol{R}) & \boldsymbol{\Delta}_{\mathrm{m}}(\boldsymbol{R}) \end{pmatrix}. \tag{7.3}$$

In the 4×4 system (6.3), $\boldsymbol{b}'$ can be formally eliminated to lowest order, giving

$$\boldsymbol{b}' = \left[-\mathbf{j}(1-\nu) + \tfrac{1}{2}(\boldsymbol{\eta}_{\mathrm{me}} + \mathbf{j}\boldsymbol{\eta}_{\mathrm{em}}\mathbf{j} - \boldsymbol{\Delta}_{\mathrm{m}}\mathbf{j} - \mathbf{j}\boldsymbol{\Delta}_{\mathrm{e}})\right]\boldsymbol{d}'. \tag{7.4}$$

After a little algebra this leads to the desired 2×2 system for $\boldsymbol{d}'$ alone,

$$2\nu\boldsymbol{d}'(\boldsymbol{R}) = \mathbf{m}_0(\boldsymbol{R})\boldsymbol{d}'(\boldsymbol{R}), \tag{7.5}$$

where

$$\mathbf{m}_0(\boldsymbol{R}) = (\boldsymbol{\Delta}_{\mathrm{e}}(\boldsymbol{R}) - \mathbf{j}\boldsymbol{\Delta}_{\mathrm{m}}(\boldsymbol{R})\mathbf{j} + \mathbf{j}\boldsymbol{\eta}_{\mathrm{me}}(\boldsymbol{R}) - \boldsymbol{\eta}_{\mathrm{em}}(\boldsymbol{R})\mathbf{j}) \equiv \begin{pmatrix} a(\boldsymbol{R}) & b(\boldsymbol{R}) \\ c(\boldsymbol{R}) & d(\boldsymbol{R}) \end{pmatrix}. \tag{7.6}$$

From the solution of (7.5) for $\boldsymbol{d}'$ and $\boldsymbol{b}'$, the fields $\boldsymbol{d}$ and $\boldsymbol{b}$ can be determined by

$$\left.\begin{aligned} \boldsymbol{d} &= \left(\mathbf{1} + \tfrac{1}{2}(\boldsymbol{\eta}_{\mathrm{em}}\mathbf{j} - \boldsymbol{\Delta}_{\mathrm{e}})\right)\boldsymbol{d}', \\ \boldsymbol{b} &= -\mathbf{j}\left(\mathbf{1} + \tfrac{1}{2}(\mathbf{j}\boldsymbol{\Delta}_{\mathrm{m}}\mathbf{j} - \mathbf{j}\boldsymbol{\eta}_{\mathrm{me}})\right)\boldsymbol{d}'. \end{aligned}\right\} \tag{7.7}$$

From this comes the relation between $\boldsymbol{d}$ and $\boldsymbol{b}$,

$$\boldsymbol{b}(\boldsymbol{R}) = -\mathbf{j}(\mathbf{1} + \boldsymbol{\mu}_0(\boldsymbol{R}))\boldsymbol{d}(\boldsymbol{R}), \tag{7.8}$$

where

$$\boldsymbol{\mu}_0(\boldsymbol{R}) = \tfrac{1}{2}(\boldsymbol{\Delta}_{\mathrm{e}}(\boldsymbol{R}) + \mathbf{j}\boldsymbol{\Delta}_{\mathrm{m}}(\boldsymbol{R})\mathbf{j} - \mathbf{j}\boldsymbol{\eta}_{\mathrm{me}}(\boldsymbol{R}) - \boldsymbol{\eta}_{\mathrm{em}}(\boldsymbol{R})\mathbf{j}) \equiv \begin{pmatrix} \alpha(\boldsymbol{R}) & \beta(\boldsymbol{R}) \\ \gamma(\boldsymbol{R}) & \delta(\boldsymbol{R}) \end{pmatrix}. \tag{7.9}$$

This formalism gives the two states whose refractive indices are close to $n=+1$, that is, in our previous notation, $\boldsymbol{d}^{(1)}$ and $\boldsymbol{d}^{(2)}$. The two lower states $\boldsymbol{d}^{(3)}$ and $\boldsymbol{d}^{(4)}$, with indices close to $n=-1$, can be found in a similar way, replacing $1/n(\boldsymbol{R}) = 1 + \nu(\boldsymbol{R})$ in (7.1) by $1/n(\boldsymbol{R}) = -1 + \nu(\boldsymbol{R})$.

To test the accuracy of the approximate formalism, we introduce a 'weakness parameter' ε, replacing the parameters p in (5.3) with

$$p \to p(\varepsilon) \equiv \{\varepsilon a_{\mathrm{e}}, \varepsilon a_{\mathrm{m}}, d, \varepsilon c, \varepsilon b, \varepsilon f\}, \tag{7.10}$$

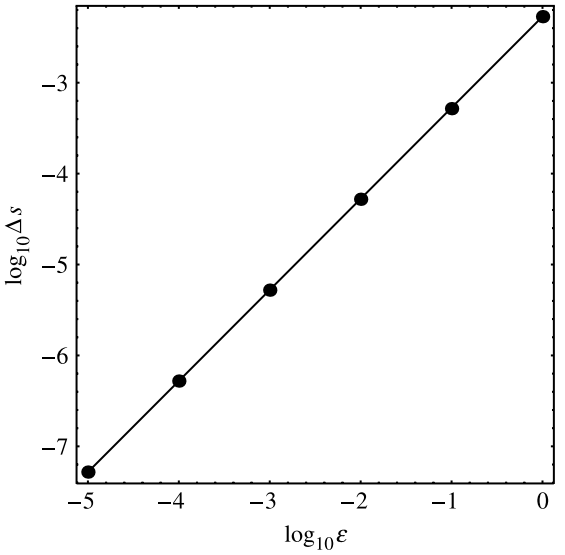

Figure 12. Dots: error $\Delta s(\varepsilon, \boldsymbol{R})$ (equation (7.13)) for the parameters of figure 1 and $\boldsymbol{R}=\{0.2, 0.3\}$, for the upper state $n^{(1)}(\boldsymbol{R})$, for $\varepsilon=10^{-n}$, $n=0, 1, 2, 3, 4, 5$; the limiting slope calculated from the data is 1.0058. Full line: theoretical error, slope=1.

whose effect is to replace the 2×2 matrix $\mathbf{m}_0(\boldsymbol{R})$ in (7.6) by

$$\mathbf{m}_0(\boldsymbol{R}) \to \varepsilon\mathbf{m}_0(\boldsymbol{R}). \tag{7.11}$$

As $\varepsilon\to0$, two of the four complex refractive indices $n(\varepsilon, \boldsymbol{R})$ approach $+1$ and two approach -1, both approaches being linear. Therefore, it is sensible to study the small $-\varepsilon$ behaviour of the eigenvalue slope, conveniently defined as

$$s(\varepsilon, \boldsymbol{R}) \equiv \frac{\mathrm{d}}{\mathrm{d}\varepsilon}|1/n(\varepsilon, \boldsymbol{R})|, \tag{7.12}$$

through the error

$$\Delta s(\varepsilon, \boldsymbol{R}) \equiv s(\varepsilon, \boldsymbol{R}) - \nu(\varepsilon, \boldsymbol{R})/\varepsilon, \tag{7.13}$$

where we have incorporated the limiting slope calculated from the approximation (7.5), whose eigenvalue ν is exactly linear in ε. As figure 12 illustrates, the error vanishes linearly as $\varepsilon\to0$, that is, the error in the indices vanishes as ε^2.

A discriminating test of the approximate theory is its ability to describe the phenomenon discussed at the end of §6 and illustrated in figure 11, of the C points and degeneracies being slightly separated for the special case of crystals without chirality (either natural optical activity or Faraday), that is, when $\mathbf{N}^{(3)}$ is symmetric. We illustrate this with the doubly anisotropic absorbing crystal (7.10), with

$$a_\mathrm{e} = 0.1, \quad a_\mathrm{m} = 0.2, \quad d = 0.3, \quad c = b = f = 0. \tag{7.14}$$

For $\varepsilon=1$ there is a degeneracy at $\boldsymbol{R}_\mathrm{D}$ and a C point (common to both electric and magnetic fields) at $\boldsymbol{R}_\mathrm{C}$, separated by $\delta\boldsymbol{R}=\boldsymbol{R}_\mathrm{C}-\boldsymbol{R}_\mathrm{D}$, given exactly (i.e. from

the 4×4 formalism) and approximately (i.e. from the 2×2 formalism (7.5)) by

$$\left.\begin{aligned}&\text{exact :}\\&\qquad \boldsymbol{R}_{\mathrm{D}} = \{0.187033, -0.7750730\},\\&\qquad \boldsymbol{R}_{\mathrm{C}} = \{0.187377, -0.7750652\},\\&\qquad \delta\boldsymbol{R} = \{3.44\times10^{-4}, 7.8\times10^{-6}\};\\&\text{approximate :}\\&\qquad \boldsymbol{R}_{\mathrm{D}} = \{0.174152, -0.7652530\},\\&\qquad \boldsymbol{R}_{\mathrm{C}} = \{0.174508, -0.7652458\},\\&\qquad \delta\boldsymbol{R} = \{3.56\times10^{-4}, 7.2\times10^{-6}\}.\end{aligned}\right\} \tag{7.15}$$

For $\varepsilon=0.1$,

$$\left.\begin{aligned}&\text{exact :}\\&\qquad \boldsymbol{R}_{\mathrm{D}} = \{0.17548556, -0.7662922354\},\\&\qquad \boldsymbol{R}_{\mathrm{C}} = \{0.17548912, -0.7662921754\},\\&\qquad \delta\boldsymbol{R} = \{3.56\times10^{-6}, 6.01\times10^{-8}\};\\&\text{approximate :}\\&\qquad \boldsymbol{R}_{\mathrm{D}} = \{0.17415204, -0.7652529729\},\\&\qquad \boldsymbol{R}_{\mathrm{C}} = \{0.17415561, -0.7652529131\},\\&\qquad \delta\boldsymbol{R} = \{3.57\times10^{-6}, 5.97\times10^{-8}\}.\end{aligned}\right\} \tag{7.16}$$

An analytical theory of the splitting is given in appendix B. For this pair of points, the formula (B 10) gives

$$\delta\boldsymbol{R} = \varepsilon^2\{3.58\times10^{-4}, 5.84\times10^{-6}\}, \tag{7.17}$$

in good agreement with (7.15) and (7.16), showing that the approximate theory is capable of describing even this very small effect.

8. Separation of electric and magnetic singularities

Because of the correction $\boldsymbol{\mu}_0(\boldsymbol{R})$ in (7.8), the electric and magnetic C and L singularities are slightly separated. To calculate the separation, we need the relation between the complex scalars w_{e} and w_{m}, defined by (3.10); from (7.8) and (7.9), this is, to lowest order,

$$w_{\mathrm{m}} = -\frac{1}{w_{\mathrm{e}}}\left(\frac{1+\alpha+\beta w_{\mathrm{e}}}{1+\delta+\gamma/w_{\mathrm{e}}}\right). \tag{8.1}$$

From (4.3), the condition for a C_{m} point is, also to lowest order,

$$w_{\mathrm{m}}^2 + 1 = 0 = -[w_{\mathrm{e}}^2 + 1 + 2(\alpha - \delta + (\gamma+\beta)w_{\mathrm{e}})]. \tag{8.2}$$

Let the C_{m} point, at $\boldsymbol{R}_{\mathrm{Cm}}$, and the nearby C_{e} point, at $\boldsymbol{R}_{\mathrm{Ce}}$, be related by

$$\boldsymbol{R}_{\mathrm{Cm}} \equiv \boldsymbol{R}_{\mathrm{Ce}} + \delta\boldsymbol{R}_{\mathrm{C}}. \tag{8.3}$$

To lowest order, the separation $\delta\boldsymbol{R}_{\mathrm{C}}$ is determined by differentiating (8.2),

$$\delta\boldsymbol{R}_{\mathrm{C}}\cdot\nabla w_{\mathrm{e}}=\frac{(\delta-\alpha)}{w_{\mathrm{e}}}-\gamma-\beta\equiv C, \tag{8.4}$$

defining the constant C, and where all quantities are evaluated at $\boldsymbol{R}_{\mathrm{Ce}}$, where $w_{\mathrm{e}}=\pm\mathrm{i}$.

The solution of the complex equation (8.4) for the real vector $\delta\boldsymbol{R}_{\mathrm{C}}$ is

$$\delta\boldsymbol{R}_{\mathrm{C}}=-2\frac{\mathrm{Im}(C^{*}\boldsymbol{s}\times\nabla w_{\mathrm{e}})}{\mathrm{Im}\ \boldsymbol{s}\cdot\nabla w_{\mathrm{e}}^{*}\times\nabla w_{\mathrm{e}}}. \tag{8.5}$$

The required ∇w_{e} can be calculated from the matrix $\mathbf{m}_0$ defined by (7.6). Some algebra leads to

$$w_{\mathrm{e}}=\pm\mathrm{i}\Rightarrow d-a=\pm\mathrm{i}(b+c)\quad\text{and}\quad\nabla w_{\mathrm{e}}=\frac{\nabla(d-a)\mp\mathrm{i}(b+c)}{b-c}. \tag{8.6}$$

(It is interesting to compare the first of these C point formulae with the condition for a degeneracy, namely $d-a=\pm 2\mathrm{i}\sqrt{bc}$.)

When the perturbation is represented as in (7.10) and (7.11), the shift $\delta\boldsymbol{R}_{\mathrm{C}}$ is proportional to ε. As a test of both the approximate theory computed numerically and the analytical formula (8.5), we choose the C_{e} and C_{m} points in figures 4*a* and 5*a*, and figures 4*b* and 5*b*, at which $w=-\mathrm{i}$. For $\varepsilon=1$, the exact and approximate points are

$$\left.\begin{aligned}&\text{exact}:\\&\qquad\boldsymbol{R}_{\mathrm{Ce}}=\{1.40462,-0.55991\},\\&\qquad\boldsymbol{R}_{\mathrm{Cm}}=\{1.42087,-0.56309\},\\&\qquad\delta\boldsymbol{R}_{\mathrm{C}}=\{0.01625,-0.00318\};\\&\text{approximate}:\\&\qquad\boldsymbol{R}_{\mathrm{Ce}}=\{1.40264,-0.54308\},\\&\qquad\boldsymbol{R}_{\mathrm{Cm}}=\{1.42164,-0.54640\},\\&\qquad\delta\boldsymbol{R}_{\mathrm{C}}=\{0.01900,-0.00332\}.\end{aligned}\right\} \tag{8.7}$$

For $\varepsilon=0.1$, the corresponding numbers are

$$\left.\begin{aligned}&\text{exact}:\\&\qquad\boldsymbol{R}_{\mathrm{Ce}}=\{1.41009,-0.54629\},\\&\qquad\boldsymbol{R}_{\mathrm{Cm}}=\{1.41187,-0.54657\},\\&\qquad\delta\boldsymbol{R}_{\mathrm{C}}=\{0.00178,-0.00028\};\\&\text{approximate}:\\&\qquad\boldsymbol{R}_{\mathrm{Ce}}=\{1.40996,-0.54469\},\\&\qquad\boldsymbol{R}_{\mathrm{Cm}}=\{1.41176,-0.54497\},\\&\qquad\delta\boldsymbol{R}_{\mathrm{C}}=\{0.00181,-0.00028\}.\end{aligned}\right\} \tag{8.8}$$

For this pair of points, the analytical formula (8.5) gives

$$\delta\boldsymbol{R}_{\mathrm{C}}=\varepsilon\{0.018001,-0.002782\}, \tag{8.9}$$

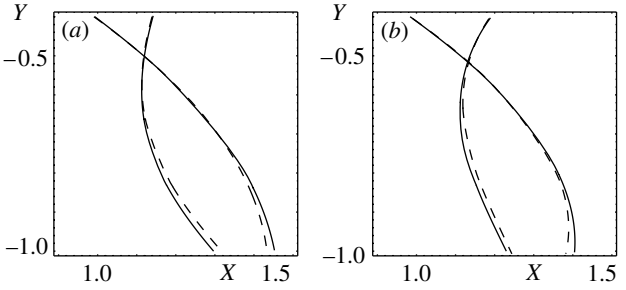

Figure 13. (*a*) L_{e} lines corresponding to figure 4*a*,*c* combined; (*b*) L_{m} lines corresponding to figure 4*b*,*d* combined. Full curves: exact 4×4 calculation; dashed curves: approximate 2×2 calculation based on (7.5).

indicating good agreement of the exact splitting with both the numerical and analytical versions of the weak-crystal approximate theory, even when ε is not very small.

The electric and magnetic L lines are similarly given accurately by the perturbation theory of §7, as illustrated in figure 13.

An analytical theory for the shift δ_{L} of the L_{m} line from the L_{e} line can be obtained by using an argument based on (4.4) and similar to that leading to (8.5). If the shift is measured in the direction of the unit vector $\boldsymbol{u}_{\mathrm{L}}$ locally perpendicular to L_{e}, that is

$$\boldsymbol{R}_{\mathrm{Lm}} \equiv \boldsymbol{R}_{\mathrm{Le}} + \delta_{\mathrm{L}} \boldsymbol{u}_{\mathrm{L}}, \tag{8.10}$$

then, after a short calculation using the fact that w_{e} is real, we obtain the result

$$\delta_{\mathrm{L}} = \frac{\mathrm{Im}[\alpha - \delta - \gamma/w_{\mathrm{e}} + \beta w_{\mathrm{e}}]}{\boldsymbol{u}_{\mathrm{L}} \cdot \boldsymbol{\nabla} \arg\, w_{\mathrm{e}}}, \tag{8.11}$$

where all quantities are evaluated at the point $\boldsymbol{R}_{\mathrm{Le}}$, on the L_{e} line, where the shift is being calculated.

9. Concluding remarks

It should be clear that general bianisotropic crystals can exhibit a rich variety of optical behaviour; even in this long paper it has been possible to give only an outline of the effects that can occur. As a guide through the complexity of crystal space, the approach based on the three types of singularity seems helpful. It is natural to ask about possible experimental manifestations of the singularities. Space prevents a discussion in this paper, so a few remarks must suffice.

As in the pure electric case, the singularities could be observed in the conoscopic figures (Berry *et al.* 1999; Berry & Dennis 2004) generated by crystal slabs sandwiched between a polarizer and an analyser and diffusely illuminated. Each type of singularity gives rise to a characteristic feature of the pattern that has been studied in detail (Berry & Dennis 2003). With bianisotropy (or even double anisotropy), the electric and magnetic C and L singularities (though not the degeneracies) are different. Observing these effects would require techniques sensitive to the electric and magnetic polarization states separately.

Perhaps the most surprising outcome of the theory is the effectiveness of the perturbation theory of §§7 and 8. Almost all the singularity phenomena can be described accurately, even when the perturbation ε is not small. The only exception seems to be possible effects, not considered here, associated with mixing of the two pairs of states (near $n=+1$ and $n=-1$). In addition to its analytical usefulness, the perturbation theory is very convenient for numerical computations.

From a more general perspective, this study can be regarded as a contribution to the field of singular optics (Nye 1999; Soskin & Vasnetsov 2001; Berry *et al.* 2004), which usually deals with waves that are not plane, and polarization C and L singularities that occur in three-dimensional position space (Nye & Hajnal 1987), rather than the plane waves and two-dimensional direction space $\boldsymbol{s}$ considered here. The position-space analogue of weak crystals is near-paraxial waves (Berry 2004*a*), for which perturbation techniques similar to those in §8 enable the separation of the electric and magnetic singularities (close together in this case) to be calculated. As emphasized in the purely electric case (Berry & Dennis 2003), the degeneracies are new singularities, characteristic of crystal optics, with no counterparts for waves propagating in isotropic media.

I thank J. H. Hannay for a helpful suggestion, M. R. Dennis for a careful reading of the paper, and three referees for suggestions that led to substantial revisions of the paper. My research is supported by The Royal Society.

Appendix A. Numerical matrices

All entries in the matrices in equation (5.1) are chosen as random numbers between -1 and $+1$, subject to the constraints listed below (cf. (2.4)–(2.6)).

Traceless symmetric matrices:

$$\left.\begin{aligned}
\boldsymbol{\Delta}^{(3)}_{\mathrm{ea}} &= \begin{pmatrix} 0.49798 & 0 & 0 \\ 0 & 0.088946 & 0 \\ 0 & 0 & -0.586926 \end{pmatrix}, \\
\boldsymbol{\Delta}^{(3)}_{\mathrm{ead}} &= \begin{pmatrix} 0.662433 & 0.114827 & 0.169887 \\ 0.114827 & -0.074150 & 0.367126 \\ 0.169887 & 0.367126 & -0.588283 \end{pmatrix}, \\
\boldsymbol{\Delta}^{(3)}_{\mathrm{ma}} &= \begin{pmatrix} 0.183092 & 0.079095 & 0.270415 \\ 0.079095 & 0.218851 & -0.508266 \\ 0.270415 & -0.508266 & -0.401942 \end{pmatrix}, \\
\boldsymbol{\Delta}^{(3)}_{\mathrm{mad}} &= \begin{pmatrix} -0.409982 & -0.263747 & -0.061998 \\ -0.263747 & 0.753255 & -0.089899 \\ -0.061998 & -0.089899 & -0.343273 \end{pmatrix}.
\end{aligned}\right\} \qquad \text{(A 1)}$$

Antisymmetric matrices:

$$\left.\begin{aligned}
\boldsymbol{\eta}^{(3)}_{\mathrm{ef}} &= \begin{pmatrix} 0 & -0.67344 & 0.046397 \\ 0.67344 & 0 & -0.026155 \\ -0.046397 & 0.026155 & 0 \end{pmatrix}, \\
\boldsymbol{\eta}^{(3)}_{\mathrm{efd}} &= \begin{pmatrix} 0 & 0.609977 & -0.044644 \\ -0.609977 & 0 & -0.045034 \\ 0.044644 & 0.045034 & 0 \end{pmatrix}, \\
\boldsymbol{\eta}^{(3)}_{\mathrm{mf}} &= \begin{pmatrix} 0 & -0.020520 & -0.784817 \\ 0.020520 & 0 & 0.466329 \\ 0.784817 & -0.466329 & 0 \end{pmatrix}, \\
\boldsymbol{\eta}^{(3)}_{\mathrm{mfd}} &= \begin{pmatrix} 0 & 0.771639 & -0.033730 \\ -0.771639 & 0 & -0.143284 \\ 0.033730 & 0.143284 & 0 \end{pmatrix}.
\end{aligned}\right\} \tag{A 2}$$

General matrices:

$$\left.\begin{aligned}
\boldsymbol{\eta}^{(3)}_{\mathrm{emc}} &= \begin{pmatrix} 0.466013 & -0.548429 & 0.970435 \\ 0.11445 & -0.685073 & -0.779722 \\ -0.784781 & -0.275784 & 0.448513 \end{pmatrix}, \\
\boldsymbol{\eta}^{(3)}_{\mathrm{emcd}} &= \begin{pmatrix} -0.830229 & -0.875759 & 0.837611 \\ 0.550703 & -0.38383 & 0.766546 \\ -0.628402 & 0.099132 & -0.354266 \end{pmatrix}, \\
\boldsymbol{\eta}^{(3)}_{\mathrm{emb}} &= \begin{pmatrix} -0.985892 & -0.78574 & 0.897604 \\ -0.520039 & 0.909896 & 0.46656 \\ 0.727833 & -0.64428 & -0.927715 \end{pmatrix}, \\
\boldsymbol{\eta}^{(3)}_{\mathrm{embd}} &= \begin{pmatrix} -0.964587 & -0.9908 & 0.035857 \\ -0.703096 & -0.014630 & 0.950773 \\ 0.021752 & -0.917356 & 0.087766 \end{pmatrix}.
\end{aligned}\right\} \tag{A 3}$$

Appendix B. Splitting of degeneracies and *C* points in the absence of chirality

We seek an approximate C point of $\boldsymbol{d}$, satisfying (4.3), i.e. $w_{\mathrm{e}} = \pm \mathrm{i}$. $\boldsymbol{d}$ is related to $\boldsymbol{d}'$ by (6.2), where $\boldsymbol{d}'$ is determined (cf. 7.5) by the matrix $\mathbf{m}_0(\boldsymbol{R})$, which is symmetric when there is no Faraday effect or natural optical activity, i.e. $b(\boldsymbol{R}) = c(\boldsymbol{R})$ in (7.6). Because of the symmetry, a degeneracy of $\mathbf{m}_0$ is also a C

point of $\boldsymbol{d}'$, where $w_{\mathrm{e}}'=\pm\mathrm{i}$. From (6.2), $\boldsymbol{d}'$ is given in terms of $\boldsymbol{d}$ to lowest order (cf. (7.2)) by

$$\boldsymbol{d}' = (1+\boldsymbol{\sigma})\boldsymbol{d}, \tag{B 1}$$

where

$$\boldsymbol{\sigma} = \tfrac{1}{2}(\boldsymbol{\Delta}_{\mathrm{e}} - \boldsymbol{\eta}_{\mathrm{em}}\mathbf{j}). \tag{B 2}$$

With the scalings (7.10) and (7.11), the components of $\boldsymbol{\sigma}$ are of order ε.

The relation between the two ws is

$$w_{\mathrm{e}}' = w_{\mathrm{e}}\left(\frac{1+\sigma_{YY}+\sigma_{YX}/w_{\mathrm{e}}}{1+\sigma_{XX}+\sigma_{XY}w_{\mathrm{e}}}\right). \tag{B 3}$$

At the desired C point, to lowest order in $\|\boldsymbol{\sigma}\|$,

$$w_{\mathrm{e}}'^2 + 1 = 2[\sigma_{XX} - \sigma_{YY} \pm \mathrm{i}(\sigma_{XY}+\sigma_{YX})]. \tag{B 4}$$

In terms of the elements (7.6) of m_0,

$$w_{\mathrm{e}}' = \frac{d-a\pm\sqrt{(d-a)^2+4b^2}}{2b}. \tag{B 5}$$

Expanding near the degeneracy $\boldsymbol{R}_{\mathrm{D}}$, defining

$$\boldsymbol{R}_{\mathrm{C}} \equiv \boldsymbol{R}_{\mathrm{D}} + \delta\boldsymbol{R}, \tag{B 6}$$

gives

$$d(\boldsymbol{R}) - a(\boldsymbol{R}) = \pm 2\mathrm{i}b(\boldsymbol{R}) + \delta\boldsymbol{R}\cdot\boldsymbol{\nabla}(d-a\mp 2\mathrm{i}b), \tag{B 7}$$

with the gradients evaluated at $\boldsymbol{R}_{\mathrm{D}}$. Then some algebra gives, to lowest order,

$$w_{\mathrm{e}}'^2 + 1 = \mathrm{i}\sqrt{\frac{\pm 4\mathrm{i}\delta\boldsymbol{R}\cdot\boldsymbol{\nabla}(d-a\mp 2\mathrm{i}b)}{b}}, \tag{B 8}$$

displaying the familiar square-root behaviour characterizing a non-Hermitian degeneracy.

Thus the desired splitting $\delta\boldsymbol{R}$ is determined from (B 4) by

$$\delta\boldsymbol{R}\cdot\boldsymbol{\nabla}(d-a\mp 2\mathrm{i}b) = \pm\mathrm{i}b[\sigma_{XX}-\sigma_{YY}\pm\mathrm{i}(\sigma_{XY}+\sigma_{YX})]^2. \tag{B 9}$$

The solution of this equation is given by (8.5) with the replacements

$$\left.\begin{aligned} &\delta\boldsymbol{R}_{\mathrm{C}} \to \delta\boldsymbol{R}, \quad w_{\mathrm{e}} \to d-a\mp 2b, \\ &C \to \pm\mathrm{i}b[\sigma_{XX}-\sigma_{YY}\pm\mathrm{i}(\sigma_{XY}+\sigma_{YX})]^2. \end{aligned}\right\} \tag{B 10}$$

All quantities are evaluated at $\boldsymbol{R}_{\mathrm{D}}$. This shows that the splitting of singularities is of order ε^2, consistent with the numerical results (7.15) and (7.16). In evaluating the result (7.17) from (B 9), use was made of the fact that in

the illustrative example chosen there was no bianisotropy (cf. (7.14)), implying that the matrix $\boldsymbol{\sigma}$ is symmetric.

References

Berry, M. V. 2004*a* The electric and magnetic polarization singularities of paraxial waves. *J. Opt. A Pure Appl. Opt.* **6**, 475–481.

Berry, M. V. 2004*b* Physics of nonhermitian degeneracies. *Czech. J. Phys.* **54**, 1040–1047.

Berry, M. V. & Dennis, M. R. 2003 The optical singularities of birefringent dichroic chiral crystals. *Proc. R. Soc. A* **459**, 1261–1292. (doi:10.1098/rspa.2003.1155.)

Berry, M. V. & Dennis, M. R. 2004 Black polarization sandwiches are nontrivial square roots of zero. *J. Opt. A Pure Appl. Opt.* **6**, S24–S25.

Berry, M. V., Bhandari, R. & Klein, S. 1999 Black plastic sandwiches demonstrating biaxial optical anisotropy. *Eur. J. Phys.* **20**, 1–14.

Berry, M. V., Dennis, M. R. & Soskin, M. S. 2004 The plurality of optical singularities. *J. Opt. A Pure Appl. Opt.* **6**. [Editorial instruction to special issue.]

Borzdov, G. N. 1990*a* Waves with quadratic amplitude dependence on coordinates in uniaxial crystals. *J. Mod. Optics* **37**, 281–284.

Borzdov, G. N. 1990*b* Waves with cubic amplitude dependence on coordinates in biaxial crystals. *Opt. Commun.* **75**, 205–207.

Borzdov, G. N. 1996 Waves with linear, quadratic and cubic coordinate dependence on amplitude in crystals. *Pramana-J. Phys.* **46**, 245–257.

Hehl, F.W. & Obukhov, Y.N. 2004 Linear media in classical electrodynamics and the Post constraint, http://arxiv.org/abs/physics/0411038.

Heiss, W. D. & Harney, H. L. 2001 The chirality of exceptional points. *Eur. Phys. J. D* **17**, 149–151.

Kong, J. A. 1974 Optics of bianisotropic media. *J. Opt. Soc. Am.* **64**, 1304–1308.

Kong, J. A. 1975 *Theory of electromagnetic waves*. New York: Wiley.

Krowne, C. M. 1984 Electromagnetic theorems for complex anisotropic media. *IEEE Trans. Antennas Propagat.* **AP-32**, 1224–1230.

Lakhtakia, A. 1998 Anomalous axial propagation in helicoidal bianisotropic media. *Opt. Commun.* **157**, 193–201.

Lakhtakia, A. 2001 Beltrami field phasors are eigenvectors of 6×6 linear constitutive dyadics. *Microw. Opt. Technol. Lett.* **30**, 127–128.

Lakhtakia, A. 2002 Conditions for circularly polarized plane wave propagation in a linear bianisotropic medium. *Electromagnetics* **22**, 123–127.

Lakhtakia, A. 2004 On the genesis of the Post constraint in modern electromagnetism. *Optik* **115**, 151–158.

Lakhtakia, A., Varadan, V. K. & Varadan, V. V. 1991 Plane waves and canonical sources in a gyroelectromagnetic uniaxial medium. *Int. J. Electronics* **71**, 1057–1062.

Mackay, T. G. & Lakhtakia, A. 2004 Negative phase velocity in a uniformly moving, homogeneous, isotropic dielectric-magnetic medium. *J. Phys. A* **37**, 5697–5711.

Nye, J. F. 1999 *Natural focusing and fine structure of light: caustics and wave dislocations*. Bristol: Institute of Physics Publishing.

Nye, J. F. & Hajnal, J. V. 1987 The wave structure of monochromatic electromagnetic radiation. *Proc. R. Soc. A* **409**, 21–36.

Pancharatnam, S. 1958 Light propagation in absorbing crystals possessing optical activity—electromagnetic theory. *Proc. Ind. Acad. Sci.* **XLVII**, 227–244.

Raab, R. E. & de Lange, O. L. 2005 Transformed multipole theory of the response fields D and H to electric octupole–magnetic quadrupole order. *Proc. R. Soc. A* **461**, 595–608. (doi:10.1098/rspa.2004.1389.)

Ramachandran, G. N. & Ramaseshan, S. 1961 In *Crystal Optics in Handbuch der Physik*, vol. XXV/I (ed. H. Flügge). Berlin: Springer.

Soskin, M. S. & Vasnetsov, M. V. (eds) 2001 Singular optics (optical vortices): fundamentals and applications. *Proc. SPIE* **4403**.

Tan, E. L. & Tan, S. Y. 2000 Concise spectral formalism in the electromagnetics of bianisotropic media. *Prog. Electromag. Res.* **25**, 309–331.

Voigt, W. 1902 On the behaviour of pleochroitic crystals along directions in the neighbourhood of an optic axis. *Phil. Mag.* **4**, 90–97.

Von Neumann, J. & Wigner, E. 1929 On the behavior of eigenvalues in adiabatic processes. *Phys. Z.* **30**, 467–470.

Weiglhofer, W. S. & Lakhtakia, A. 2003 *Introduction to complex mediums for optics and electromagnetics*. Bellingham, WA: SPIE Press.

As this paper exceeds the maximum length normally permitted,
the author has agreed to contribute to production costs.